

IDENTIFYING MULTIPLE REFLECTIONS WITH THE NIP AND NORMAL HYPOTHETICAL WAVEFRONTS

J.C.R. Cruz, P. Chira, and F. de Souza

email: *jcarlos@ufpa.br*

keywords: *interbed symmetric multiple reflections, NIP wave, N wave, NMO velocity, forward modeling, Kirchhoff migration*

ABSTRACT

The multiple reflections include in the seismograms important informations about the reflectors in subsurface and can become completely invisible. In marine data acquisition the water layer behaves as a wave trap, where the waves are repeatedly reflected at the sea surface and sea bottom without significant amplitude loss. In order to identify and locate target reflectors, these multiples must be eliminated or, at least, attenuated. In this work, interbed symmetric multiple reflections were identified in synthetic dataset. We compare the parameters of hypothetical wavefronts Normal-Incidence-Point (NIP) and Normal (N) obtained by forward modeling and Kirchhoff migration. This comparison was extended to consider the Normal-Moveout (NMO) velocity. These comparisons led us to identify and differentiate between multiple and primary reflections.

INTRODUCTION

Seismograms include multiple reflections that can be so strong that the desired primary reflections become completely invisible. In marine data the water layer often behaves like a wave trap and the waves are repeatedly reflected at the sea surface and sea bottom without significant amplitude loss. Then, the identification and localization of a target-reflector, which might indicate for instance an oil reservoir requires that multiple reflections must be eliminated or attenuated (Zaske, 2000). An important task in the seismic processing is the identification and consequent suppression of multiple reflections.

According to Trappe et al. (2001) the multiple suppression does not necessarily require conventional processing. Alternatively, low velocity zones, that are attributed to multiples, can be edited in the velocity field derived from Common-Reflection-Surface (CRS) parameters. The CRS method is macro-velocity model independent. It stacks the amplitudes of seismic traces in multicoverage data along a surface defined by CRS traveltimes approximation which fits best the data set. This technique has been applied on synthetic and real data with successful results, showing to be more efficient than the conventional processes, e.g. Common-Midpoint (CMP) or Normal-Moveout/Dip-Moveout (NMO/DMO) stack.

Maciel (2001) simulated first-order zero-offset (ZO) multiple reflections using the CRS method for a forward modeling. The strategy used is based on the knowledge of the model and includes a recursive process to calculate the radius of curvature of the NIP and Normal (N) wavefronts, respectively (Hubral, 1983).

Gamboa (2003) applied an algorithm to identify the CRS parameters of primary reflections in seismic data. After this, it was attenuated or eliminated the not desired energy (multiple). He obtained the CRS parameters of the multiple reflections from the corresponding parameters of the primary reflections. The results were successful.

Maciel et al. (2005) applied the multichannel Wiener-Levinson (WL) Deconvolution method in real data in CRS domain to attenuate multiple reflections due to reverberation in water depth and at the top and bottom of the salt pillow and still the presence of peg-legs. They obtained successful results where the primary

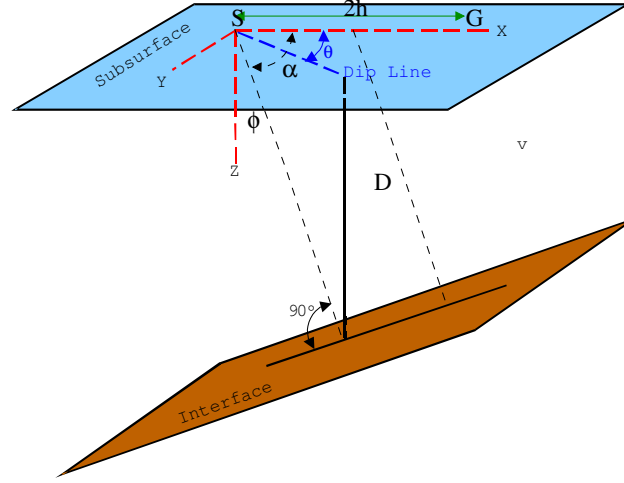


Figure 1: 3-D model showing the relations between the angles α , ϕ and θ (modified from Levin (1971)).

reflections are good determined.

In this work, we identify first-order interbed symmetric multiple reflections for a simple 2-D synthetic model. A comparison was done between the parameters of NIP and N wavefronts obtained by forward modeling and by using Kirchhoff migration. This comparison also was extended for NMO velocity. Through these comparisons it is possible to identify multiple and primary reflections.

TRAVELTIME APPROXIMATION FOR MULTIPLE REFLECTIONS

It is considered a model in depth consisting of a layer over a half-space, separated by a dipping and a plane reflector (Figure 1). In this case, the root-mean-square (rms) velocity, the interval velocity and average velocity are the same. It is assumed that there is a constant velocity v between the ground surface and the reflector.

The n -order multiple reflection traveltimes for the 3-D case is given by (Levin, 1971)

$$t_n^2 = \left(\frac{2D \sin(n+1)\phi}{v \sin \phi} \right)^2 + 4 \left(\frac{1 - \cos^2 \theta \sin^2(n+1)\phi}{v^2} \right) h^2, \quad (1)$$

where n is the order of the multiple. For the primary reflection, $n = 0$. The offset between the source S and the receiver G is given by $2h$. The angle between the normal to the reflector and the profile is given by α . ϕ is a direction cosine of the normal to the plane. D is the distance from a point along the profile, halfway between the source S and geophone G . The dip angle of the interface is given by θ (Figure 1).

Substituting $\theta = 0$ in equation (1) then we obtain for a 2-D model the representation of the n -order multiple reflection traveltimes given by (Levin, 1971)

$$t_n^2 = \left(\frac{2D \sin(n+1)\phi}{v \sin \phi} \right)^2 + 4 \left(\frac{1 - \sin^2(n+1)\phi}{v^2} \right) h^2. \quad (2)$$

The stacking velocity v_{NMO_n} is defined by

$$v_{NMO_n} = \frac{v}{\sqrt{1 - \sin^2(n+1)\phi}}. \quad (3)$$

Another way to represent the NMO velocity is given by

$$v_{NMO} = \frac{2v R_{NIP}}{t_0 \cos^2 \beta_0}. \quad (4)$$

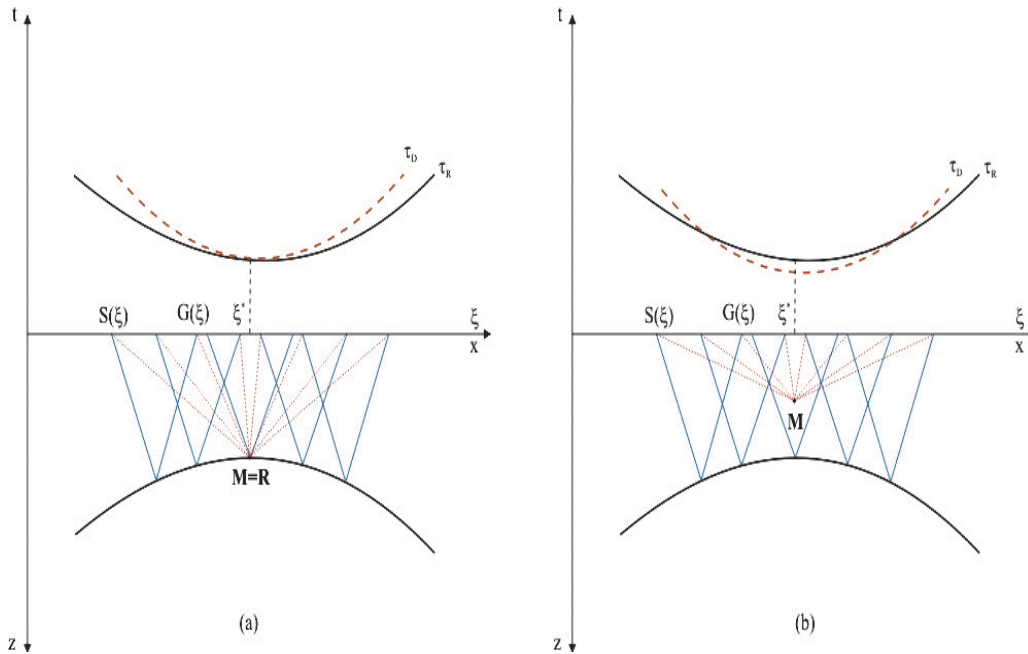


Figure 2: 2-D representations of the 3-D traveltime surfaces, t_R and t_D for different chosen points M in depth (from Schleicher et al. (1993)).

From NMO velocity also we can express the rms velocity given by

$$v_{rms}^2 = v_{NMO}^2 \cos^2 \beta_0 = \frac{2v R_{NIP}}{t_0} . \quad (5)$$

being β_0 the emergence angle of the normal ray (coincident source and receiver). R_{NIP} is the radius of curvature of the NIP wave and t_0 is the two-way ZO traveltime.

GENERAL ASSUMPTIONS ABOUT KIRCHHOFF MIGRATION

Seismic migration searches the relation between the diffraction curve and the position of a diffractor point, where any sample can be related to a point in subsurface, whose representation corresponds to a diffraction curve. The migration process stacks the amplitudes of seismic traces that coincide with the migration curve, fixing the result in the apex of this curve. This operation is repeated for all the samples of a seismic section. In this work we use the Kirchhoff type migration, which considers that all the points of the subsurface are potential candidates to belong to reflectors.

It is assumed a plane and horizontal measurement surface, $z = 0$, with source-receiver (S, G) pairs represented by (Schleicher et al., 1993)

$$x_S = x_S(\xi) , \quad x_G = x_G(\xi) , \quad (6)$$

where ξ is a parameter in surface that identifies the position of a source-receiver pair. The seismic primary reflections from the searched-for reflector are described for each pair (S, G) by zero-order ray theory. They fall on the called reflection time curve, t_R . Connecting each point S and G with an arbitrary depth point M (Figure 2) provides the diffraction traveltime curve or Huygens curve (t_D) for that point, along which a diffraction stack is performed. These curves are tangent if and only if $M = R$ (Figure 2). A diffraction stack performed with arbitrary weights along the Huygens curve will provide a nonzero contribution when $M = R$. Otherwise the result will be negligible (Schleicher et al., 1993).

Diffraction Stack

Schleicher et al. (1993) define for all points ξ within aperture \hat{A} and for each fixed subsurface point M (Figure 2) the diffraction traveltime curve given by

$$\tau_D(\xi, M) = \tau(S, M) + \tau(M, G), \quad (7)$$

where $\tau(S, M)$ and $\tau(M, G)$ denote the traveltimes from $S(\xi)$ to M and from M to $G(\xi)$, respectively. All diffraction stacks are based on performing a weighed summation along the Huygens τ_D curve with respect to each point M . This summation can be mathematically expressed by the following integral (Schleicher et al., 1993)

$$V(M, t) = \frac{1}{\sqrt{2\pi}} \int_A d\xi w(\xi, M) \dot{U}(\xi, t + \tau_D(\xi, M)), \quad (8)$$

where the value $V(M, t = 0)$ is the diffraction stack migration output for the chosen depth point M . Integral (8) is the ‘‘time differentiated, space-weighted Kirchhoff migration’’ (Schleicher et al., 1993). The expression $\dot{U} = dU/dt$, where U is the analytic particle displacement. The diffraction stack is employed to represent diffraction traveltime curves τ_D along of which the summation is performed. $w(\xi, M)$ denotes the weight function.

After some considerations and little changes in equation (8) the asymptotic value of the diffraction stack integral modified into the frequency domain ω is represented by

$$\hat{V}_F(M, \omega) = \hat{V}(M, \omega)F(\omega) \approx \hat{W}(\omega)w(\xi^*, M) \frac{R_c A}{\mathcal{L}\sqrt{|\mathcal{H}_F|}} e^{i\omega\tau_F(\xi^*, M) + \frac{i\pi(\text{sgn } H_F - 1)}{4}}, \quad (9)$$

where $\hat{W}(\omega)$ and $\hat{V}(M, \omega)$ denote the Fourier transforms of $W(t)$ and $V(M, t)$, respectively. $W(t)$ represents the analytic point-source wavelet. $F(\omega)$ is a filter and is represented by $\sqrt{-i\omega}$. R_c is the plane-wave reflection coefficient at the reflection point R . The total loss in amplitude due to transmissions across all interfaces along the ray is represented by A . \mathcal{L} is the normalized geometrical spreading factor. $H_F = (\partial^2 \tau_F(\xi, M)/\partial \xi^2)|_{\xi=\xi^*} \neq 0$, where τ_F is the phase function. ‘‘Sgn’’ is the signature function.

Application to synthetic data

We consider a simple 2-D acoustic model constituted of two homogeneous layers above a half-space, separated by two interfaces, one curve and other plane-horizontal. The interval velocities from top to bottom are 2.5 km/s, 3.5 km/s and 4.5 km/s for the half-space (Figure 3)

Using the ray-tracing software SEIS88 (Červený and Psensik, 1988) were generated the multicoverage synthetic data. These data contains primary reflections and first-order symmetrical multiple reflections only for the first reflector. To obtain the parameters of hypothetical waves, NIP and N, a forward ZO section was simulated. This section is constituted by 51 seismic traces (Figure 4). The source signal was a Gabor wavelet with 40 Hz dominant frequency and the time sampling was 2 ms.

To recover the true depth of the reflectors the Kirchhoff migration algorithm was applied. For this migration it was adopted a target zone $0 \leq x \leq 4$ km and $0 \leq z \leq 3$ km with $\Delta x = 0,01$ km and $\Delta z = 0,015$ km. The migrated seismic image is showed in Figure 5. We observe in this Figure a good recovery of the reflectors in depth and the presence of artifacts, as consequence of the migration process. The presence of one third reflector is also observed and corresponds the first-order symmetrical multiple reflection of the first reflector. Figure 6 represents a ZO seismic section of the migrated model. In this Figure it is observed the absence of the second reflector. That is due to fact that there is no contrast of seismic impedance between the second and third layer of the model because the layers have the same properties (e.g. velocity, density). The third layer of the migrated model appears due to the presence of the multiple reflection of the first reflector.

The accurate values of the three parameters of the hypothetical waves and the NMO velocity have been calculated by forward modeling. These values were compared with its corresponding values obtained by the migrated model using in both cases the software SEIS88. The estimated values correspond to the positions of the maximum amplitude of each seismic signal. We observed that the values of the parameters

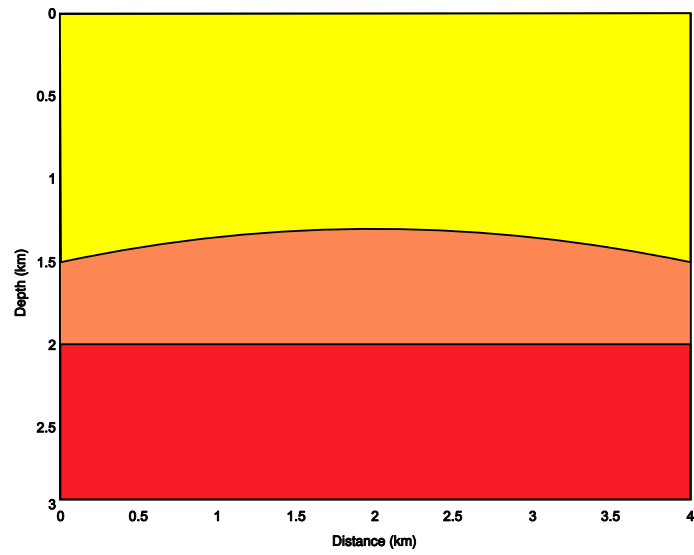


Figure 3: 2-D model constituted by two layers above a half-space.

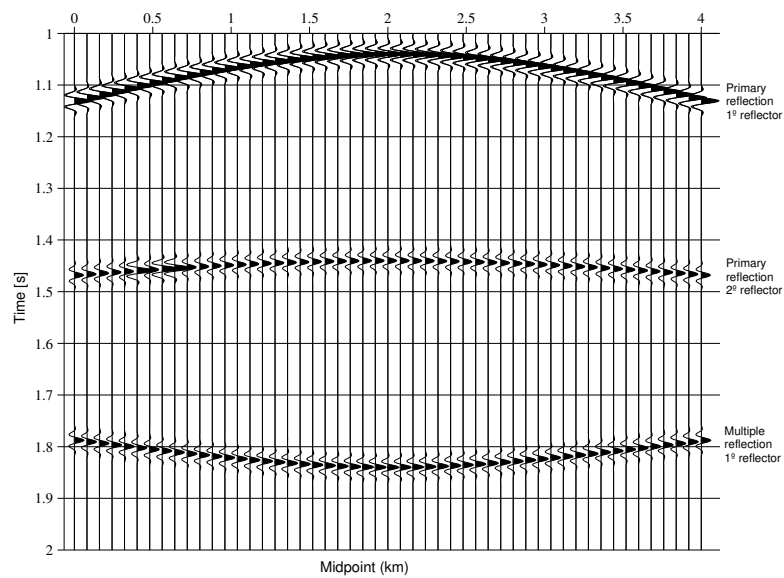


Figure 4: ZO seismic section modeled with the software SEIS88.

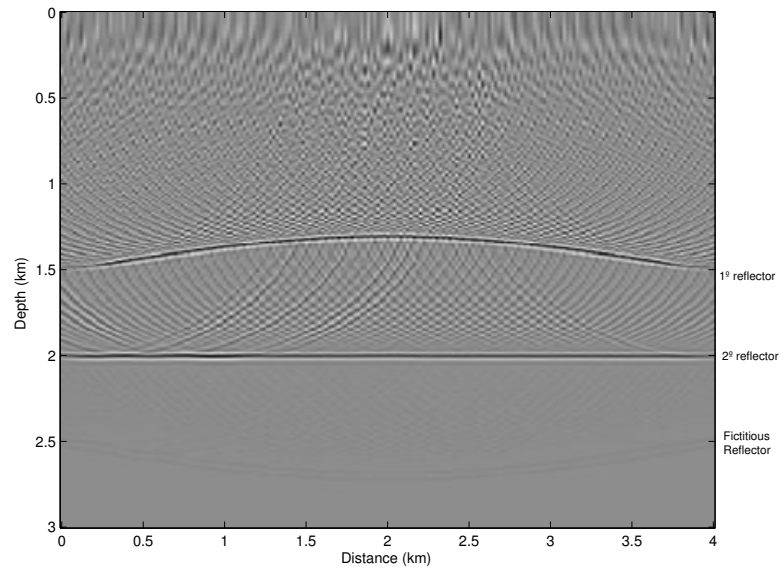


Figure 5: Migrated section using the Kirchhoff process. It is observed a third reflector or fictitious reflector that corresponds to the multiple reflections.

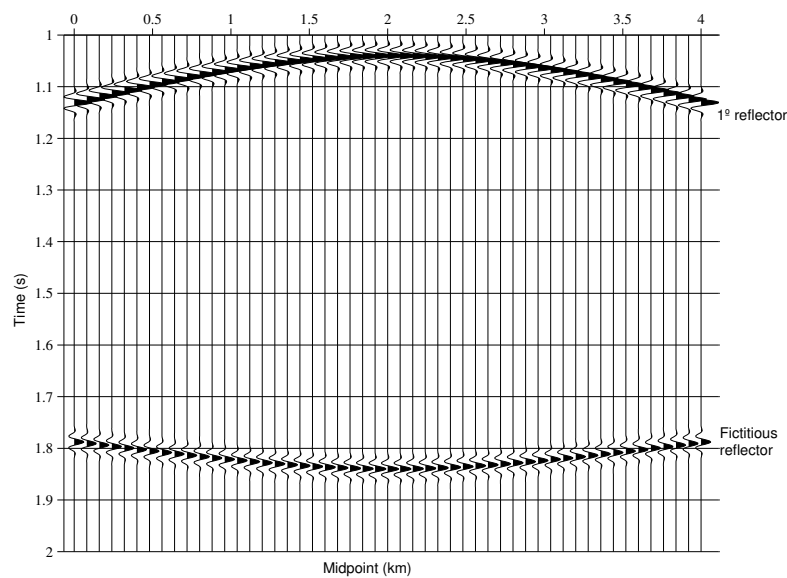
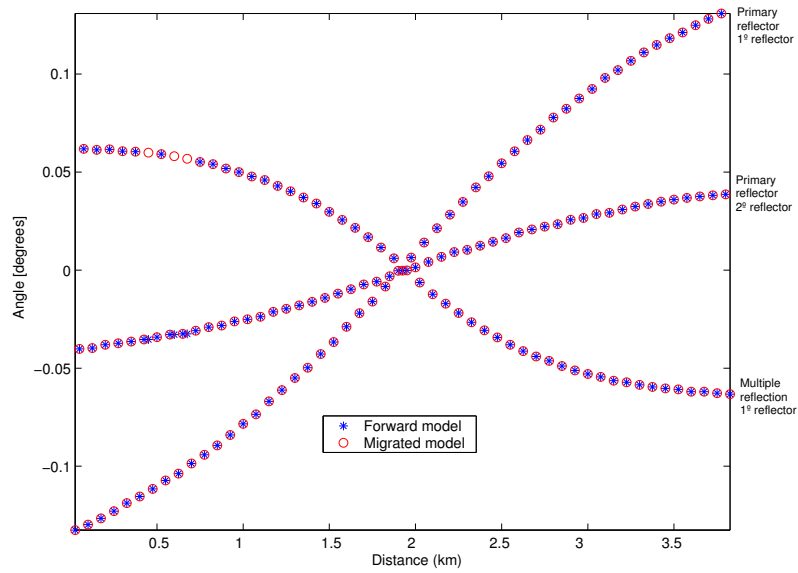
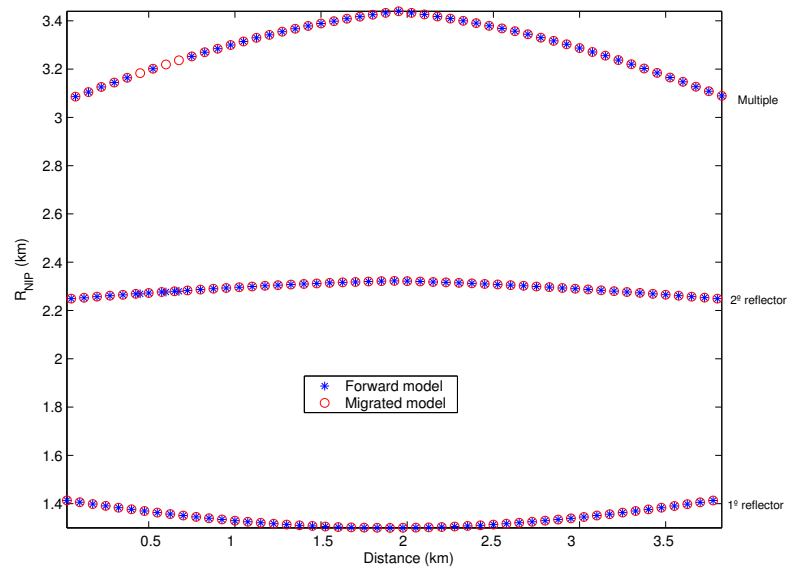


Figure 6: ZO seismic section modeled of Figure 5. It is observed the absence of the plane interface, which functions as a mirror, and the presence of the third interface (fictitious), that is a specular image of the first interface.



(a)



(b)

Figure 7: Comparison of the NIP wavefront parameters between the forward model and the migrated model in depth (Kirchhoff method): a) emergence angle of the normal ray, β_0 , b) radius of curvature of the NIP wavefront, R_{NIP} .

of hypothetical (NIP and N) waves and NMO velocity for the forward model are similar to the same parameters for the migrated model (Figures 7 and 8). The values of parameters R_{NIP} and V_{NMO} are bigger when compared with the primary reflections (Figures 7b and 8b) due to the multiple path to be bigger with respect to the primary reflection path.

CONCLUSIONS

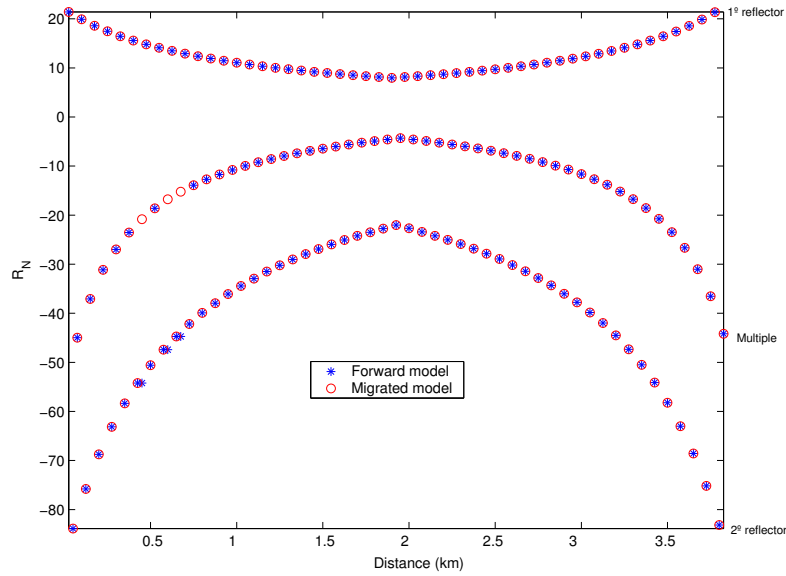
In these initial results multiple reflections were identified due to the following indicatives: a) absence of acoustic impedance in the migrated model because the densities between the second and third layer are equal, b) there is symmetry of the radius of curvature of the N wave between the first and “last reflector” (Figure 8a). This is verified by the comparison of parameters ($\beta_0, R_{NIP}, R_N, V_{NMO}$) between the forward model and the migrated model. In this way, was confirmed the presence of the multiple reflections in the seismic section. These indicatives are very important and can be considered in seismic interpretation .

ACKNOWLEDGMENTS

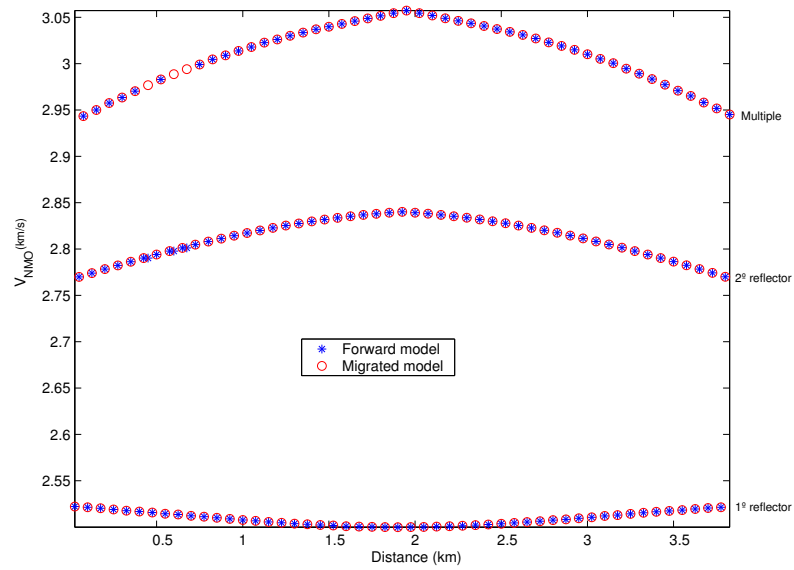
This work was kindly supported by the sponsors of the *Wave Inversion Technology (WIT) Consortium*, Karlsruhe, Germany.

REFERENCES

- Červený, V. and Psensik, I. (1988). Ray tracing program. *Charles University, Czechoslovakia*.
- Gamboa, F. (2003). Caracterização e eliminação de Múltiplas pelo Método de Superfície de Reflexão Comum (CRS). *Master thesis, State University of Campinas, Brazil (in Portuguese)*.
- Hubral, P. (1983). Computing true amplitude reflections in a laterally inhomogeneous earth. *Geophysics*, 48:1051–1062.
- Levin, F. K. (1971). Apparent velocity from dipping interface reflections. *Geophysics*, 36:510–516.
- Maciel, R. (2001). Simulação de Reflexões Múltiplas usando o Método de Empilhamento Superfície de Reflexão Comum. *Master thesis, Federal University of Pará, Brazil (in Portuguese)*.
- Maciel, R., Porsani, M., and Garabito, G. (2005). Estratégias para combinar o filtro de Wiener-Levinson multicanal com o método CRS para atenuação de reflexões múltiplas. *II Workshop da Rede Cooperativa de Pesquisa em Risco Exploratório em Petróleo e Gás, Belém-Brazil*.
- Schleicher, J., Tygel, M., and Hubral, P. (1993). 3-D True Amplitude finite-offset migration. *Geophysics*, 58(8):1112–1126.
- Trappe, H., Pruesmann, J., and Gierse, G. (2001). Case studies potential of Common Reflection Surface stack - structural resolution in the time domain beyond the conventional NMO/DMO stack. *First Break*, 19:625–633.
- Zaske, J. (2000). Identification and Attenuation of Multiple Reflections using Wafront Characteristics. *Ph.D. Thesis, University of Karlsruhe, Germany*.



(a)



(b)

Figure 8: Comparison of the Normal (N) wavefront parameter and the NMO velocity between the forward model and the depth migrated model (Kirchhoff method); a) radius of curvature of the Normal wave, R_N , and b) NMO velocity, V_{NMO} .